

Finding numerically Newhouse sinks near a homoclinic tangency and investigation of their chaotic transients

Takayuki YAMAGUCHI

(Received March 13, 2013; Revised November 27, 2013)

Abstract. For Hénon map of nearly classical parameter values, we search numerically for Newhouse sinks. We show how to find successively the Newhouse sinks of higher period, which is the estimation of coordinates of the sinks from power laws of properties of the sinks, and investigate numerically a sequence of sinks of period from 8 to 60 that we obtained. We also show how to verify the existences of obtained sinks by interval arithmetic. The sinks of period from 8 to 14 from among our obtained sinks was verified mathematically.

In the case that we observed, when the sink exists, most orbits converge to it, and the orbit that seems to be Hénon attractor is not an attractor but just a long chaotic transient. The narrowness of the main bands of basins of the sinks causes the long chaotic transients. We also investigate numerically the chaotic transients and their rambling time.

Key words: Newhouse sink, homoclinic tangency, chaotic transient.

1. Introduction

In this paper we investigate numerically Newhouse sinks of Hénon map. Our numerical result shows the properties of Newhouse sinks and reveals that the appearances of Newhouse sinks in our cases cause the changes from Hénon attractor to a long chaotic transient. Firstly, we show how to seek Newhouse sinks. In general, simple iterations of some initial points converge to an attractor. It is difficult for simple iterations of some initial points to find Newhouse sinks because the parameter ranges in which these sinks exist are too short. Our search for a sequence of Newhouse sinks consists of two main steps: the search of the first few Newhouse sinks by using algorithm based on implicit function theorem and the estimation of parameters and coordinates of the succeeding Newhouse sinks. Secondly, we verify our obtained sinks by applying Brouwer fixed point theorem with interval arithmetic and show numerical data of power laws of the sequence of the sinks. Thirdly, we discuss the chaotic transients of these sinks.

We deal with a sequence of sinks that are constructed to prove coexistence of infinitely many sinks. Newhouse showed coexistence of infinitely many sinks when a one-parameter family of two dimensional dissipative diffeomorphism creates a homoclinic tangency nondegenerately [11], [12]. There exist a horseshoe in a neighborhood of a homoclinic tangency near the parameter that the homoclinic tangency occurs. When we perturb the parameter, a periodic point in the horseshoe becomes stable. Such a sinks at different parameters compose a sequence converging to the homoclinic tangency, which is our object in this paper. In addition, because of abundance of diffeomorphisms having a homoclinic tangency, infinitely many sinks coexist near the parameter of the homoclinic tangency.

The convergence of the aforementioned sequence to the homoclinic tangency means the following. If a one parameter family $\{F_t\}$ of two dimensional dissipative diffeomorphisms has a homoclinic tangency, there is a sequence of parameters $\{t_j\}$ accumulating to the parameter value of the tangency such that the diffeomorphism F_{t_j} has a sink q_j of period n_j and, as j varies to infinity, the sequence of sinks $\{q_j\}$ accumulates to the point of the tangency and the sequence n_j goes to infinity [6], [11], [13]. We refer to the sequence of sinks as an infinite cascade of sinks. This phenomenon gives the existence of a diffeomorphism with a sink of arbitrarily high period near a diffeomorphism having a homoclinic tangency.

Each sink in an infinite cascade of sinks is constructed as below. Perturbing a diffeomorphism with a homoclinic tangency, we can construct a horseshoe near the homoclinic tangency. To be more precise, we can take a rectangle region near the homoclinic tangency in an appropriate coordinate such that some iterations of the diffeomorphism transfer the rectangle back to its neighborhood and the image of the rectangle is bent and has two intersections with the rectangle. As the parameter varies to the homoclinic tangency the horseshoe are destroyed. Full horseshoe, that is, a situation so that the intersection of the rectangle and its image consists of two components, has two saddle periodic points. As the parameter varies slightly so as to break the full horseshoe of the dissipative diffeomorphism, one of the two saddles becomes stable. As the parameter varies further to the tangency, the subsequent horseshoes appear and destroy in turn. One sink appears in each horseshoe and these sinks in the horseshoes constitute the cascade.

We deal with only such sinks that appear in the horseshoes in a neighborhood of a homoclinic tangency, which are called “simple” Newhouse sinks

and are investigated in [15]. The “simple” Newhouse sinks are defined as the sinks having their orbits consisting of the following two parts: one part near the saddle fixed point mapped by almost linear map and the other part mapped by a nonlinear map. It is known that the parameter range of coexistence of only infinite “simple” Newhouse sinks has zero measure. Therefore, it is not easy that we find parameters of “simple” Newhouse sinks and we need the estimation described in the following sections.

We consider Hénon map [8]:

$$T_{a,b}(x, y) = (1 + y - ax^2, -bx). \tag{1}$$

It is shown in [5], [1] that the stable and unstable manifolds of the saddle fixed point $(0.631\dots, -0.189\dots)$ have a homoclinic tangency for the parameter a near 1.3924198079 when we fix $b = -0.3$. We deal with the same homoclinic tangency in the following sections.

An infinite cascade of sinks is governed by power laws [4], [13], [14]. We translate the power laws to estimations of parameters and coordinates of sinks by using calculation of stable and unstable manifolds of a fixed point. In the result, our numerical search obtained a sequence of sinks of

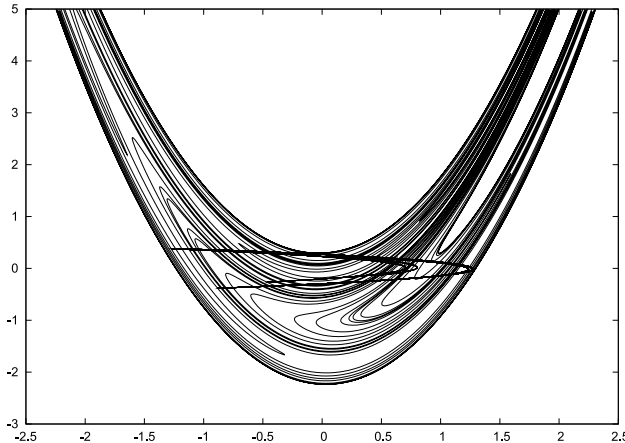


Figure 1. The stable and unstable manifolds of the saddle fixed point $(6.32536\dots, 0.18976\dots)$ of Hénon map with $a = 1.3927060035$ and $b = -0.3$ near which a homoclinic tangency occurs. The stable manifolds are the vertically long curves, which are u-shaped and reach to the top of the figure. The unstable manifolds are the horizontally long curves in the rectangle $[-1.5, 1.5] \times [-1, 1]$, which are bow-shaped and twine Hénon attractor.

period from 8 to 60. We show numerical values of the power laws satisfied by these sinks. Moreover, we verified mathematically the existences of the sink of period from 8 to 14 by numerical constructions of inclusions in a neighborhood the sinks. The verification is performed by using interval arithmetic.

We also concerned with the basins of the sinks. In particular, for the obtained sinks, our numerical investigation shows that the basins of the sinks have intersections with the unstable manifold of the saddle fixed point. Therefore, when the sink exists, the Hénon attractor loses its stability and orbits of most initial points in phase space converge to the sink near the homoclinic tangency. Our numerical investigation presents an example such that Hénon attractor that numerical experiments show to us is not an attractor but just a long chaotic transient. In addition, our numerical investigation indicates that because the width of main band of the basin of the sink of high period is very narrow a truncation error of computation hides the existences of the sinks. It is known that the parameter range of simple Newhouse sink is short and actually our numerical search for simple Newhouse sinks needs the parameter estimation. Accordingly, it is unlikely that all Hénon attractors that we can observe by numerical experiments are long chaotic transients. For chaotic transients, Buszko and Stefański investigated transients of sinks of lower period and showed the relation of sizes of periodic windows and average rambling times [3]. We apply the same analysis of [3] for sinks of lower period to the transients of the obtained sinks. It is shown that our sinks have the same properties as the sinks of lower period in point of average rambling time.

A feature of our numerical investigation is to use multiple precision library. Our computation can show finer structure of the system than computations with double precision. The numerical result in the following sections are obtained by computations whose precision is increased up to 12000 bit if needed.

The construction of this paper is the following. In Section 2 we state the definitions and settings and recall the theorem that there is an infinite cascade of sinks near a homoclinic tangency. In Section 3 we show the basins of attraction in neighborhoods of the first a few sinks. In Section 4 we state how to estimate the positions and parameters of a cascade of sinks. In Section 5, as an application of Brouwer fixed theorem, we show how to construct inclusions in neighborhoods of the sinks and verify the

sinks of period from 8 to 14. We also show numerical values of power laws of the cascade of the sinks. In Section 6 we deal with chaotic transients caused by our infinite cascade of sinks and investigate their rambling time. In appendix, an algorithm to search for first a few sinks, pseudo code of the algorithm, lists of the coordinates and parameters of the obtained sinks are shown.

The source code that we used to search for the cascade of sinks is available at the repository <https://gitlab.com/math-numerical-experiment/math-henon-tangency>.

2. Notation and settings

In this section, we recall the construction of Newhouse sink according to [13]. We consider a discrete dynamical system of a diffeomorphism F on \mathbf{R}^2 . Let $DF(p)$ denote the derivative of F at p . A point p is called a periodic point of period n if $F^n(p) = p$ and $F^i(p) \neq p$ for $0 < i < n$. In particular, a periodic point p of period 1 is called a fixed point. A periodic point p is called a sink if the absolute values of all eigenvalues of $DF(p)$ are less than one. A periodic point p is called a saddle periodic point if the two eigenvalues λ and μ of $DF(p)$ satisfy $|\lambda| < 1$ and $|\mu| > 1$. In addition, the periodic point p is called a dissipative periodic point if $|\det DF(p)| = |\lambda\mu| < 1$. We define the stable manifold $W^s(p, F)$ and the unstable manifold $W^u(p, F)$ of a saddle fixed point p of F ;

$$W^s(p, F) := \{x \in \mathbf{R}^2 \mid |f^n(p) - p| \rightarrow 0 \text{ as } n \rightarrow \infty\} \quad (2)$$

$$W^u(p, F) := \{x \in \mathbf{R}^2 \mid |f^n(p) - p| \rightarrow 0 \text{ as } n \rightarrow -\infty\}. \quad (3)$$

It is known that if F is a C^r diffeomorphism then these invariant manifolds are C^r curves and tangent to the eigendirections of $DF(p)$ at p . We call a point q a homoclinic point if q is in both $W^s(p, F)$ and $W^u(p, F)$. The homoclinic point q is called a homoclinic tangency if $W^u(q, F)$ and $W^s(q, F)$ are tangent at q . Otherwise, we call q a transverse homoclinic point.

The existence of an infinite cascade of sinks is formulated by the following theorem.

Theorem 2.1 ([13]) *Let $\{F_t : \mathbf{R}^2 \rightarrow \mathbf{R}^2\}$ be a one parameter family of C^1 diffeomorphisms depending continuously on t . Assume $\{F_t\}$ creates a homoclinic intersection at t_0 for the dissipative fixed point p_t . That is, there*

is some $\epsilon > 0$ such that for $t_0 - \epsilon < t < t_0 + \epsilon$ the subarcs $\gamma_t^s \subset W^s(p_t, F_t)$ and $\gamma_t^u \subset W^u(p_t, F_t)$ depending continuously on t satisfy the following condition:

- (1) $\gamma_t^s \cap \gamma_t^u = \emptyset$ for $t_0 - \epsilon < t < t_0$ (respectively, $t_0 < t < t_0 + \epsilon$),
- (2) for $t_0 < t < t_0 + \epsilon$ (respectively, $t_0 - \epsilon < t < t_0$), there are two transverse intersections of γ_t^s and γ_t^u and the directions at the two intersections are different from each other.

Then there is a sequence of parameters t_j converging to t_0 such that F_{t_j} has a sink of period n_j and n_j diverges for $j \rightarrow \infty$. Moreover, $\{n_j\}$ satisfies $n_{j+1} - n_j = 1$ for all j if F_t preserves the orientations on $W^s(p_t, F_t)$ and $W^u(p_t, F_t)$. Otherwise, $n_{j+1} - n_j = 2$ for all j .

Let us describe the situation of the theorem (Fig. 2). Let λ_t and μ_t be the two eigenvalues of $DF_t(p_t)$. We assume that $0 < \lambda_t < 1$ and $\mu_t < -1$. This settings are similar to the case of Hénon map (1) for the parameters $a \approx 1.3924198079$ and $b = -0.3$, which is numerically investigated in the following sections. We consider the case such that $\gamma_t^s \cap \gamma_t^u = \emptyset$ for $t_0 - \epsilon < t < t_0$ and there are transverse intersections of γ_t^s and γ_t^u for $t_0 < t < t_0 + \epsilon$. Let u_0 be the point of the tangency; $W^s(p_{t_0})$ is tangent to $W^u(p_{t_0})$ at u_0 . We also let v_0 be $F_{t_0}^{-N}(u_0)$ for some integer $N > 0$. We consider sufficiently small neighborhood U of p_t and assume that F_t is linear in U . Transforming

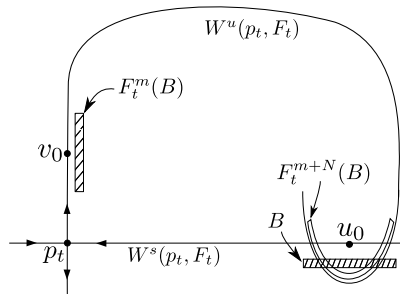


Figure 2. The situation of simple Newhouse sink. Perturbing the diffeomorphism F_{t_0} of a homoclinic tangency, we obtain the box B and the horseshoe region $F_t^{m+N}(B)$ near the point of the tangency u_0 . The diffeomorphism F_t is linear in the neighborhood of the saddle fixed point p_t ; F_t^m makes the box B shrink horizontally and stretch vertically. We obtain the rectangle $F_t^m(B)$ near v_0 . F_t^N maps a neighborhood of v_0 to a neighborhood of u_0 ; this map is nonlinear and pulls the rectangle $F_t^m(B)$ across B . The $B \cap F_t^{m+N}(B)$ includes two saddle periodic points of period $m + N$. One of these two saddles becomes stable when the parameter varies to the homoclinic tangency.

coordinate, we assume $F_t(x, y) = (\lambda_t x, \mu_t y)$ in U . We replace u_0 and v_0 by $F_{t_0}^{m_1}(u_0)$ and $F_{t_0}^{-m_2}(v_0)$ respectively for some integers m_1, m_2 , if necessary, and we let u_0 and v_0 be in U , because u_0 and v_0 are a homoclinic point of F_{t_0} . Also we assume $p_t = (0, 0)$, $u_t = (x_0, 0)$, and $v_t = (0, y_0)$ for simplicity.

We take a box $B = \{(x, y) \mid |x - x_0| \leq \delta^s, \delta_1^u \leq y \leq \delta_2^u\}$ near u_0 for $\delta^s, \delta_1^u, \delta_2^u \geq 0$. Because F_t is linear in U , the box B shrinks horizontally and stretches vertically by some iterations of F_t . We obtain a box $F_t^m(B)$ near v_0 for some integer m . Let N be an integer such that a neighborhood of v_0 is mapped to a neighborhood of u_0 by N iterations of F_t . Then $F_t^{m+N}(B)$ is a thin region having horseshoe shape parallel to $W^u(p_t, F_t)$. For suitable $\delta^s, \delta_1^u, \delta_2^u$ and m , $F_{t_1}^{m+N}(B) \cap B$ consists of two components for some parameter t_1 . Two saddle periodic points of period $m + N$ exist in $F_{t_1}^{m+N}(B) \cap B$ (Fig. 3). When the parameter t approaches to t_0 , $W^u(p_t, F_t)$ moves to the tangency point u_0 . Eventually for the parameter t_2 smaller than t_1 , $B \cap F_t^{m+N}(B)$ is the empty set. There is a parameter t between t_1 and t_2 such that one saddle periodic point of period $m + N$ becomes stable.

To obtain a sink of period $m' + N$ higher than $m + N$, we take a suitable box B' closer to $W^s(p_t, F_t)$ than the box B , in which case $F_t^{m'}(B')$ is also closer to v_0 than $F_t^m(B')$. Similarly to the case of the box B , we obtain a sink of period $m' + N$ from the box B' . We remark that the above-mentioned two sinks that are constructed from B and B' do not coexist because the sink of period $m' + N$ exists at the parameter closer to the tangency than that of the sink of period $m + N$. Taking boxes closer to $W^s(p_t, F_t)$ in turn, we obtain a sequence of sinks approaching to the point of the tangency. If the eigenvalue μ_t is negative then there are two cascades of sinks for $t_0 > t$ and for $t_0 < t$ respectively. The periods of all sinks in the sequence for $t_0 > t$ are even and the periods for $t_0 < t$ are odd, or vice versa.

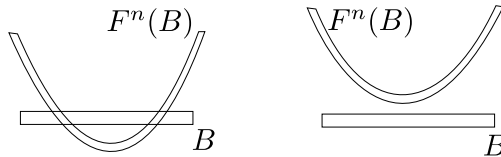


Figure 3. The left case is the situation such that each of two components of $F^n(B) \cap B$ includes one saddle periodic point. The right case is the situation such that no periodic point exists in $F^n(B) \cup B$. If F^n is dissipative, in the process of destruction of the horseshoe, that is, in the transformation from the left case to the right case, one of the two saddle periodic points obtains stability.

3. Basin of attraction for a sink near a homoclinic tangency

We show locally and globally basins of attraction of the first few Newhouse sinks. We deal with the Hénon map (1) of which the parameter b is -0.3 and the parameter a is varied in the neighborhood of 1.4 . The determinant of $DT(x, y)$ equals b , that is, -0.3 and this system is dissipative.

We sketch our procedure to obtain the first few sinks. Firstly, our investigation searches a parameter range including the parameter of a homoclinic tangency. We fix the value of the parameter a and calculate the stable and unstable manifolds of the fixed point (Fig. 1). We repeat the calculations with subtle changes of the parameter a and specify the parameter range that includes an occurrence of a homoclinic tangency (Fig. 4). Furthermore, we bisect the range of parameter a including the homoclinic tangency and obtain the narrower parameter range

$$[1.39241980792391250304093437105, \\ 1.39241980792391250304093437106]. \quad (4)$$

Next, we seek coordinates of sinks and their parameters, by using the algorithm in Appendix A.1, which is based on implicit function theorem. We obtained sinks of periods 13, 15, and 17 as a consequence of our computation. In the rest of this section, we focus on these sinks and their basins. To obtain sinks of higher period we use the estimation in Section 4.

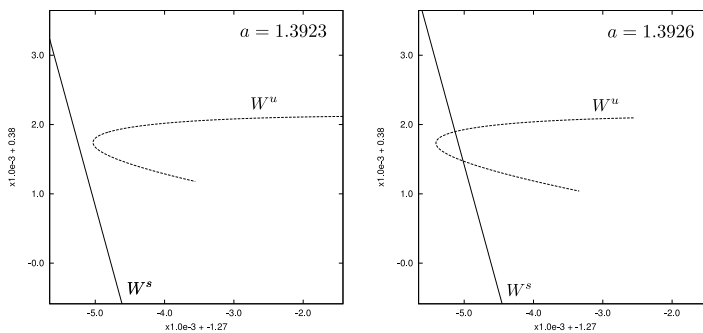


Figure 4. The segments of the stable and unstable manifolds for the saddle fixed point of Hénon map (1). The parameter b is constant and -0.3 . The left image is the case that the parameter a is 1.3923 and the homoclinic tangency has not yet occurred. The right image is the case that the parameter a is 1.3926 and the two homoclinic points exist after the homoclinic tangency.

Fig. 5 shows the orbit of the sink of period 13 and the stable and unstable manifolds of the saddle fixed point. The orbit starting from the point 0 in the figure goes to the saddle fixed point along the stable manifold and returns to the point 0 along the unstable manifold. The figure ensures that the situation of the sink is the same as that of the last section.

The basin of attraction of the sink of period 13 are shown in Fig. 6. The basin is narrow and the main band of basin has a scale of 10^{-7} near the point 0 in 5. The basin is too long to determine numerically the length of

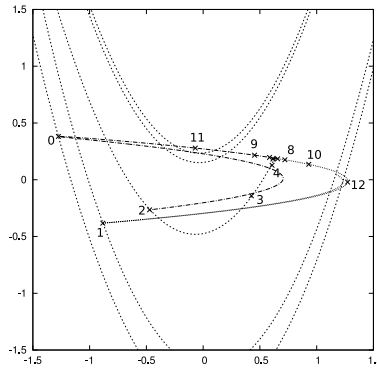


Figure 5. The orbit of the sink of period 13 and the stable and unstable manifolds for the saddle fixed point. The orbit starting from the point denoted by 0 moves along the stable manifold at first. After passing through the saddle fixed point the orbit moves along the unstable manifold with reversal because the eigenvalue of unstable direction for the saddle fixed point is negative.

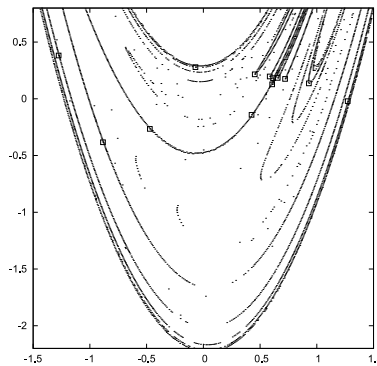


Figure 6. The main band of basin of attraction for the orbit of sink of period 13 denoted by \square . We could not finish the numerical calculation of the boundary of basin; the length of boundary does not seem to be finite.

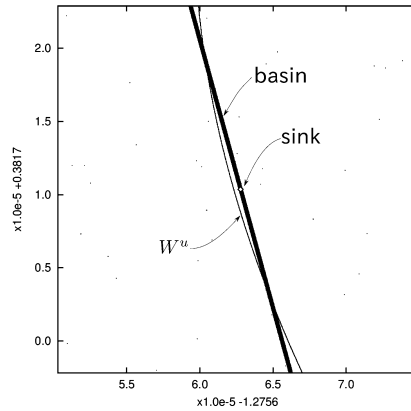


Figure 7. Magnification near the sink of period 13, where the sink is denoted by the diamond at the center. The thick line is basin of attraction and the thin and curved line is unstable manifold W^u of the fixed point. There are two intersections of the basin band and the unstable manifold.

basin boundary and does not seem to have finite length. We are interested in the existence of Hénon attractor when the sink exists. Fig. 7 shows that the basin of attraction has the intersection with the unstable manifold. The closure of the unstable manifold of the saddle fixed point includes Hénon attractor. Therefore, most points in the phase space get through the orbit like Hénon attractor and eventually converge to the sink. In other words, there are the chaotic transients like the Hénon attractor (Fig. 9). We discuss the transients in Section 6.

From the view of bifurcation, this sink is created through saddle-node bifurcation and proceeds to period-doubling bifurcation [16]. The period-doubling bifurcation is terminated by the crisis; the attractor arising from period-doubling bifurcation collides with the saddle periodic point of period 13. Similarly to [7] the boundary of basin of the sink of period 13 consists of the stable manifold of the saddle fixed point of period 13, where both of the sink and the saddle are simultaneously born at the saddle-node bifurcation.

Finally, we show the movements of the stable and unstable manifolds, the sinks of period 13, 15, and 17, and their basins of attraction (Fig. 8). The figure shows the region near the sink denoted by 0 in Fig. 5. When the parameter a decreases from about 1.3927 to the parameter value of the homoclinic tangency, the stable manifold moves to right and the unstable manifold moves to left; then these manifolds approaches to the tangency. In

the next section, we estimate the position of the sink from the move of the stable and unstable manifolds.

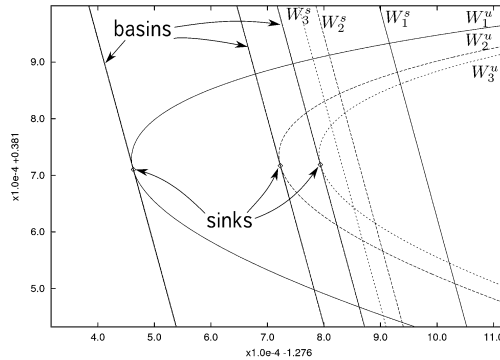


Figure 8. The movements of sinks, their basins of attraction, and the stable and unstable manifolds of the fixed points when the parameter a changes. The lines W_1^s and W_1^u are the stable and unstable manifolds of the fixed point for $a = 1.39270603828125$. Similarly, W_2^s and W_2^u are the stable and unstable manifolds for $a = 1.392497593643890380859375$, and W_3^s and W_3^u are the stable and unstable manifolds for $a = 1.3924409549236297607421875$. When the parameter a increases, the stable manifold moves from left to right and the unstable manifold moves from right to left. The sinks exist near the peaks of the unstable manifolds and these basins are lines parallel to each stable manifold. Starting from the left of figure, the periods of the sinks are 13, 15, and 17, respectively.

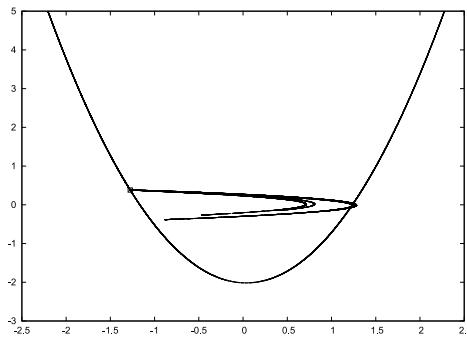


Figure 9. A chaotic transient and a stable manifold of a saddle of period 13 at $a = 1.3927060035$ and $b = -0.3$. \square is the sink of period 13. The orbit like Hénon attractor is a transient orbit. After sufficiently large iterations (about 150000 iterations on the average), most orbits converge to the sink of period 13.

4. Estimation of positions of sinks

In this section, we show an algorithm to obtain the succeeding sinks of a cascade from the first few sinks and the stable and unstable manifolds of the fixed point.

We recall the known results on the asymptotic behavior and the power laws of the parameters of a cascade of sinks. We consider the situation of the Theorem 2.1 and for simplicity assume that the two eigenvalues λ_t and μ_t are positive. The relation between the parameters and the unstable eigenvalue at the saddle fixed point is shown in [4], [13];

$$\lim_{n \rightarrow \infty} \frac{t_n - t_{n-1}}{t_{n+1} - t_n} = \mu_{t_0},$$

where t_n is the parameter value that the sink of period n exists and t_0 is the parameter of homoclinic tangency. This fact enables us to estimate the parameter value t_{n+1} from the last two parameter values t_{n-1} and t_n .

The relations of bifurcation parameters are described in [14] as

$$\lim_{n \rightarrow \infty} \frac{\bar{t}_n - t_0}{\bar{t}_{n+1} - t_0} = \lim_{n \rightarrow \infty} \frac{\tilde{t}_n - t_0}{\tilde{t}_{n+1} - t_0} = \mu_{t_0},$$

where the saddle-node bifurcation creates the two periodic points of period n at \bar{t}_n , one of the periodic points changes its stability at \tilde{t}_{n+1} through period-doubling bifurcation, and t_0 is the parameter of the homoclinic tangency. We also are interested in the range of parameter such that a sink exists. The evaluation in [15] gives

$$\lim_{n \rightarrow \infty} \frac{\bar{t}_n - \tilde{t}_n}{\bar{t}_{n+1} - \tilde{t}_{n+1}} = \mu_{t_0}^2.$$

To apply these relations to our case such that the unstable eigenvalue is negative, we replace the diffeomorphism F_t by F_t^2 ;

$$\lim_{n \rightarrow \infty} \frac{t_n - t_{n-2}}{t_{n+2} - t_n} = \mu_{t_0}^2, \tag{5}$$

$$\lim_{n \rightarrow \infty} \frac{\bar{t}_n - t_0}{\bar{t}_{n+2} - t_0} = \lim_{n \rightarrow \infty} \frac{\tilde{t}_n - t_0}{\tilde{t}_{n+2} - t_0} = \mu_{t_0}^2, \tag{6}$$

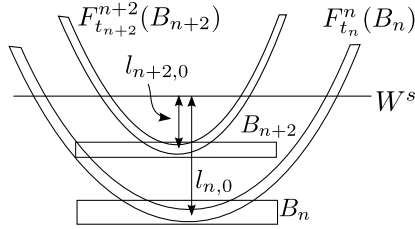


Figure 10. The situation that B_n and B_{n+2} include the sinks of period n and $n + 2$ respectively. Then the relation (8) for $l_{n,0}$ and $l_{n+2,0}$ is satisfied. Note that the parameter t_n such that B_n includes a sink is different from the parameter t_{n+2} such that B_{n+2} includes a sink.

$$\lim_{n \rightarrow \infty} \frac{\bar{t}_n - \tilde{t}_n}{\bar{t}_{n+2} - \tilde{t}_{n+2}} = \mu_{t_0}^4. \tag{7}$$

To find sinks numerically we want to estimate the positions of the sinks. In our case, because the unstable eigenvalue μ_t is negative, an infinite cascade of sinks is split into two sequences by the stable manifold: a sequence of even period on one side and a sequence of odd period on the other side. The estimation in such a situation is to obtain the approximate position of the sink of period $n + 2$ from the position of the sink of period n for Hénon map $F_t = T_{t,-0.3}$. The position of the box B in Fig. 2 relates to the position of stable manifold of the fixed point as below. Let B_n be the box including the sink of period n and $l_{n,i}$ be the distance between the stable manifold and the center point of $F_t^i(B_n)$ for an integer $i \geq 0$. The boxes B_n and B_{n+2} are mapped to a neighborhood of v_0 and F_t is approximately linear in the neighborhood of the saddle fixed point. We obtain $l_{n,i} = |\mu_t|^{-i} l_{n,0}$. Let k be an integer such that $F_t^k(B_n)$ is in a neighborhood of v_0 . Then $F_t^{k+2}(B_{n+2})$ must be in a neighborhood of v_0 and $l_{n,k} = l_{n+2,k+2}$ holds. Therefore, we obtain the relation on the positions of two boxes including the sinks,

$$\frac{l_{n,0}}{l_{n+2,0}} = \mu_t^2. \tag{8}$$

The relation (8) does not take into account the condition that one of the two periodic points in the box is stable. We remember Fig. 3 and consider the intersection of the box and the horseshoe when the periodic point is stable. If the intersection of B_n and $F_{t_n}^n(B_n)$ is composed of two

components, both of two periodic points of period n are saddle. If the intersection is empty then there is no periodic point. Therefore, at some parameter that the intersection is composed of one component, one of the two periodic points is stable. The horseshoe region created by n iterations of the box B_n is narrow and is close to the unstable manifold of the fixed point. Consequently, the unstable manifold approximates to the horseshoe region and the sink is near the peak of the unstable manifold (Fig. 8). Let \bar{l} be the distance between the stable manifold and the peak of the unstable manifold. We can regard \bar{l} as $l_{n,0}$ for the parameters such that the sinks exist. We search for the parameter satisfying

$$\frac{l_{n,0}}{\bar{l}} = \mu_t^2 \quad (9)$$

and the obtained parameter is the estimation of parameter such that a sink exists. We can also regard the peak of the unstable manifold from the stable manifold as the estimation of position of the sink.

From the first three sinks of period 13, 15, and 17 mentioned in Section 3. we obtained eventually the sinks of period 8 to 60. For example, the procedure to obtain the sink of period 19 from the two sinks of period of 15 and 17 is as below. We calculate the distance $l_{17,0}$ between the sink of period 17 and the stable manifold. Applying (5) to the two sinks of period 15 and 17, we obtain the first estimation of the parameter for the sink of period 19. To refine the estimation further, we search for the parameter such that the condition (9) holds from the calculations of the stable and unstable manifolds near the first estimation of parameter. We obtain the final estimation of the parameter in this way and also obtain the position of the peak of the unstable manifold at the parameter. Fixing both a parameter in a neighborhood of the estimation of the parameter and an initial point in a neighborhood of the peak point of unstable manifold, we test a convergence of simple iteration. If the convergent point is found then it is a sink of period 19. For the sinks of higher period, we repeat the above procedure.

5. Verification of sinks and power law

By using the estimation described in the last section, our computer program searched for sinks of odd period and sinks of even period, respectively. As a result, we obtained a sequence of sinks of period from 8 to 60. The

coordinates, parameters, and eigenvalues of the obtained sinks are listed in the tables in Appendix A.3. In this section, we deal with verification of the sinks and power laws of some properties of the sinks.

First, we verify the existences of these sinks. To prove the existences of the periodic points, we combine Brouwer fixed point theorem with interval arithmetic. We also check that the periodic points are sinks by calculating enclosures of eigenvalues at the periodic points. We can verify the existences of the sinks of period from 8 to 14, whose data is shown in Table 1.

Interval arithmetic is a method that defines operations on set of intervals and deals with rounding errors on computers nicely. We consider an interval enclosing a number instead of the number itself. When some arithmetic operations produce a resultant number, we calculate intervals enclosing the number instead of calculating the approximation of the number. Endpoint numbers of intervals on computers are numbers that is represented rigorously by floating point numbers and rounding errors of digital computation are brought into extra expansions of resultant intervals. It is mathematically rigorous that the interval calculated by interval arithmetic on computers is an interval enclosing true value.

We recall properties of functions on interval arithmetic [10]. For intervals I_1 and I_2 , we define arithmetic operations by

$$I_1 \circ I_2 = \{x \circ y \mid x \in I_1, y \in I_2\},$$

where \circ is $+$, $-$, or \times . When $0 \notin I_2$, we define I_1/I_2 by

$$I_1/I_2 = I_1 \times (1/I_2),$$

where $1/I_2 = \{1/x \mid x \in I_2\}$. Identifying $x \in \mathbb{R}$ with $[x, x]$, we regard x as an interval. Two-dimensional interval vectors, that is, pairs of intervals, correspond to two-dimensional vector. For any continuous map $f : \mathbb{R}^2 \rightarrow \mathbb{R}^2$, we consider an interval extension of f written by \bar{f} ; it is defined as an interval vector valued map that satisfies $\bar{f}([x, x], [y, y]) = f(x, y)$ for any $(x, y) \in \mathbb{R}^2$. We note that we can not determine f uniquely from the definition. Just replacing real numbers in the map (1) by intervals, we extend it to an interval valued map;

$$\bar{T}_{A,B}(X, Y) = (1 + Y - AX^2, -BX), \quad (10)$$

Table 1. The data of verified periodic points: the ranges of x -coordinate, y -coordinate, parameter a , and two eigenvalues, where α and β are two eigenvalues at the periodic points. The ranges of x -coordinate and y -coordinate are coordinates of four corners of minimum rectangles that include images of inclusions obtained by our numerical construction. When the parameter b is -0.3 and the parameter a is in the specified range, a periodic point exists in the ranges of x -coordinate and y -coordinate and the periodic points are sinks because the absolute values of the eigenvalues are less than one.

| | | |
|----------|----------|--|
| 8 | x | $[-1.2641480315599056, -1.2641480315599057]$ |
| | y | $[0.3815883095535991, 0.3815883095535990]$ |
| | a | $[1.3866414978735625, 1.3866414978735626]$ |
| | α | $[-0.0001317565296413, -0.0001317565296411]$ |
| | β | $[-0.4979639352876563, -0.4979639352876542]$ |
| | 9 | x |
| y | | $[0.3815001609062766, 0.3815001609062765]$ |
| a | | $[1.3968296778150859, 1.3968296778150860]$ |
| α | | $[0.0000393390430422, 0.0000393390430427]$ |
| β | | $[-0.5003426234527945, -0.5003426234527932]$ |
| 10 | | x |
| | y | $[0.3817739305802194, 0.3817739305802193]$ |
| | a | $[1.3904445108073844, 1.3904445108073845]$ |
| | α | $[-0.0000118133309073, -0.0000118133309067]$ |
| | β | $[-0.4998505541313075, -0.4998505541313065]$ |
| | 11 | x |
| y | | $[0.3816834340024865, 0.3816834340024864]$ |
| a | | $[1.3934818331832507, 1.3934818331832508]$ |
| α | | $[0.0000035426394508, 0.0000035426394519]$ |
| β | | $[-0.5000424187451586, -0.5000424187451572]$ |
| 12 | | x |
| | y | $[0.3817369729481438, 0.3817369729481437]$ |
| | a | $[1.3918712413591354, 1.3918712413591355]$ |
| | α | $[-0.0000010629383349, -0.0000010629383331]$ |
| | β | $[-0.4999735008295995, -0.4999735008295976]$ |
| | 13 | x |
| y | | $[0.3817101619053220, 0.3817101619053219]$ |
| a | | $[1.3927060351470881, 1.3927060351470882]$ |
| α | | $[0.0000003188573829, 0.0000003188573864]$ |
| β | | $[-0.5000113143693783, -0.5000113143693747]$ |
| 14 | | x |
| | y | $[0.3817242881938740, 0.3817242881938739]$ |
| | a | $[1.3922705183540199, 1.3922705183540200]$ |
| | α | $[-0.0000000956602776, -0.0000000956602712]$ |
| | β | $[-0.4999953250901844, -0.4999953250901780]$ |

where A , B , X , and Y are intervals. Because the map (1) is polynomial, it is known that the following fact;

$$T_{A,B}(X, Y) \subset \bar{T}_{A,B}(X, Y), \quad (11)$$

where the left-hand side is an image of the map T and the right-hand side is a value of the interval extension \bar{T} .

From Brouwer fixed point theorem, if we construct a rectangle that is mapped back into itself by n iterations and has no intersections with images of m iterations for $0 < m < n$. an existence of a periodic point of period n is guaranteed. Our sinks do not have such rectangle neighborhoods because the directions of eigenvectors at the sinks are close and there are parts of the rectangle that are away from the sinks transiently. In general, points sufficient close to a sink approach monotonically to the sink for directions of eigenvectors at the sink, but points in a rectangle neighborhood do not always approach monotonically to the sink in the distance of the orthogonal coordinate. To construct an inclusion on a rectangle, we consider coordinate change from the orthogonal coordinate to the coordinate of the eigenvectors at the sink. We take a small rectangle R around the origin and map R to a neighborhood of the sink by a linear transform g , which maps the origin to the sink and x-axis and y-axis to the eigendirections of the sink. After iterating R by $T_{a,b}$, we restore the coordinate by g^{-1} and we check $g^{-1} \circ T_{a,b} \circ g(R) \subset R$. Because the linear transform g is a homeomorphism, if $g^{-1} \circ T_{a,b} \circ g$ has a periodic point in R then $T_{a,b}$ has a periodic point in $g(R)$.

From 11, we obtain the following relation for interval extensions \bar{g} , \bar{g}^{-1} , and $\bar{T}_{A,B}$;

$$g^{-1} \circ T_{a,b} \circ g(R) \subset \bar{g}^{-1} \circ \bar{T}_{A,B} \circ \bar{g}(R), \quad (12)$$

where A and B are intervals satisfying $a \in A$ and $b \in B$. Therefore, if we find a rectangle R such that

$$\bar{g}^{-1} \circ \bar{T}_{A,B} \circ \bar{g}(R) \subset R, \quad (13)$$

then Hénon map $T_{a,b}$ has periodic points in $g(R)$. However, in our case, size of a rectangle increases approximately twofold at each iteration of $\bar{T}_{A,B}$ and $\bar{g}^{-1} \circ \bar{T}_{A,B} \circ \bar{g}(R)$ become too large rectangle so that R can not include

it. To obtain finer enclosure of $g^{-1} \circ T_{a,b} \circ g(R)$, we need to subdivide a rectangle into small rectangles before each iteration. The value of an interval extension for a rectangle is defined as a union of values for subdivided small rectangles. In other words, for a polynomial f and an interval vector V that is represented by a union of some interval vectors $V = \cup_i^N V_i$, we obtain from (11)

$$f(V) \subset \bigcup_i^N \bar{f}(V_i). \tag{14}$$

Therefore, we can replace the left-side hand of (13) by such unions obtained by subdividing rectangles every mapping step. Subdivisions causes increase of amount of computation. For that reason, the verification for sinks of high period are very hard and we constructed only inclusions for the sinks of period 8 to 14.

We show results of the verification. Fig 11 shows a neighborhood of the sink of period 13. The left figure is the region enclosing the sink of period 13, the right figure is the region mapped by 13 iterations of the map, and the former covers the latter. Table 1 shows the data obtained from the verification's. We state the verification's for the sinks of period 8 to 14 as a proposition.

Proposition 5.1 *Hénon map (1) has the periodic points of period 8 to 14 in the ranges of parameter a , x -coordinate and y -coordinate listed in Table*

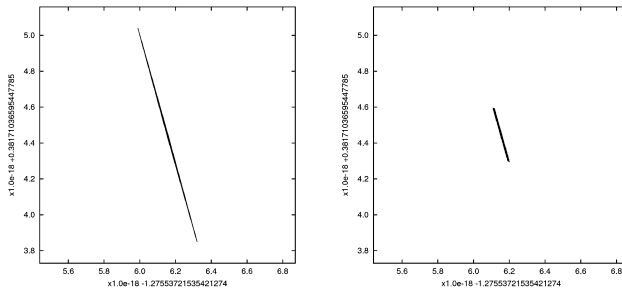


Figure 11. Regions such that the iteration of 13 times maps the region in the left figure to the region in the right figure. The regions are composed small rectangle regions. The iteration for each small rectangle region are calculated by interval arithmetic. From this data of the two regions, we obtained that the iteration of 13 times of Hénon map is an inclusion on the region in the left figure and a periodic point of period 13 exists.

1, when $b = -0.3$. The absolute values of the eigenvalues at the periodic points are less than one. The periodic points are stable.

We make sure known power laws of the cascade of sinks (5) and (8). We calculate the sizes of parameter intervals of periodic windows and the distances between stable manifolds and peaks of unstable manifolds. Fig. 12 shows that these values are governed by the power law. The shrinking ratio of the sizes of periodic windows is square of eigenvalue at the fixed point for unstable direction and the distances between the stable manifolds and the peaks of the unstable manifolds get smaller by absolute value of unstable eigenvalue at the fixed point.

We are interested in the properties of basins. As stated previously, the basins of the obtained sinks are most of phase space except points that go to infinity. However, in practice, there are points with long transients and points with short transients, of course, which is not rigorous distinction. The basins composing points with short transients are bands parallel to the stable manifolds shown in Fig. 8. For some parameters we calculated such basins, but we could not observe radical change in neighborhoods of the sinks. As a sort of size of the basin, we consider width in a neighborhood of the sink. We calculate two basin boundaries in a neighborhood of the sink and we regard minimum distance between the two boundaries as the width

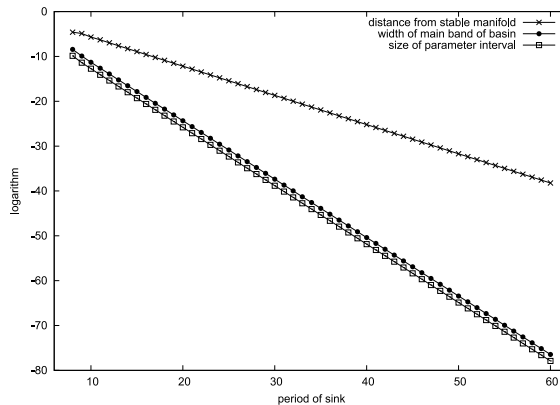


Figure 12. Logarithm of distance between peak of unstable manifold and stable manifold of a fixed point, logarithm of width of main band of basin, and logarithm of size of parameter interval that a sink exists. The slopes are about -0.650612 , -1.30444 , and -1.30478 , which agree with $\log|\mu_{t_0}| \approx 0.65130925$ and $\log|\mu_{t_0}^2| \approx 1.3026185$.

of the basin. The calculated result is shown in Fig. 12; the shrinking ratio of the widths of basins is the square of eigenvalue.

We describe the difficulty of finding sinks of high period in the cascade of sinks. For example, for the sink of period 27, the size of parameter interval is about 6.6×10^{-15} and the width of the basin of attraction is about 7.9×10^{-14} . It seems to be difficult for the calculation with double precision (53 bit) to find the sink of period larger than 27. Even if the precision is sufficient large, it is difficult that numerical investigation finds the sinks of higher period. There are two reasons; the basin of attraction is narrow and the parameter interval that a sink exists is short. The width of the basin of the sink of period $n + 2$ is about 7% of that of the sink of period n . The size of the parameter interval of the sink of period n is about 7.4% of that of the sink of period n . If we search for the sink of period $n + 2$ in the same region to the region of period n with finer step, we must calculate about 200 ($\approx 1/(0.07 \times 0.074)$) times as much as the case of period n . Therefore, to obtain a sequence of sinks, we need the above mentioned estimations of positions and parameters of sinks.

6. Chaotic transients

The appearances of simple Newhouse sinks found by our computer program cause chaotic transients, which are chaotic behaviors before the orbits converge to a periodic attractor. In our case, chaotic transients are orbits like the Hénon attractor before they converge to simple Newhouse sinks, which is shown in Fig. 9. In this section, we investigate these chaotic transients. At the beginning, we review known results related to chaotic transients. Subsequently, we show the analysis for average rambling times of our cascade of sinks.

Firstly, we review influence of simple Newhouse sinks to a chaotic attractor. Tatjer and Simó proved under some conditions that when a simple Newhouse sink exists the closure of the unstable manifold of the saddle fixed point includes the sink [14]. In that case, a chaotic attractor does not exist in the closure of the unstable manifold of the saddle fixed point. In particular, the Hénon attractor does not exist. The numerical investigation in this paper seems to give a specific case of [14, Theorem 5.8], but it is not clear that the condition of the theorem holds because it is difficult to calculate numerically some of values in the condition.

Secondly, we review studies of rambling time, which is an iteration number needed for an orbit to enter a neighborhood of a periodic point. To begin with, we need to define a suitable neighborhood of a periodic point to determine rambling time. For example, Jacobs et al. considered a quadratic map $y = a - x^2$ and defined an immediate basin as below. Let x_s and x_u be two fixed points; $x_s = (-1 + \sqrt{1 + 4a})/2$ and $x_u = (-1 - \sqrt{1 + 4a})/2$. For a parameter a such that x_s is stable, an immediate basin is defined as an interval $[x_u, -x_u]$. Buszko and Stefański also defined a black subset as a union of intervals whose orbits monotonically approach a periodic point [2].

Because rambling time depends on its initial point, we take a lot of uniformly distributed initial points in phase space and we consider the average of rambling time. For one-dimensional quadratic maps, Jacobs et al. showed numerically in [9] that, for a given parameter where a periodic point is stable, the average rambling time scales with the size of periodic window including the parameter;

$$\tau \sim \Delta a^{-1/2},$$

where τ is the average rambling time and Δa is the size of the periodic window of parameter space. Moreover, for Hénon map with small b , they approximated Hénon map by a logistic map and conjectured

$$\tau \sim \Delta a^{1/2-d}, \quad (15)$$

where d is a fractal dimension of Hénon attractor. In [3], for Hénon map with $b = -0.3$, the average rambling time for windows of low period exhibits the same type scaling as (15),

$$\tau \sim \Delta a^{-\beta}, \quad (16)$$

where β is a constant determined by numerical calculation and $\beta = 0.9 \pm 0.1$.

In the rest of this section, we apply the same analysis in [3] and investigate the same type scaling of average rambling time for the obtained sinks. First of all, we state the definition of rambling time at an initial point and how to determine a threshold value that is required to calculate rambling time. In our numerical investigation, the definition of the rambling time of an initial point for a stable periodic point is simply the minimum number of

iterations that the distance from the sink becomes less than an appropriate threshold value. In other word, we take an appropriate threshold distance d for a stable periodic point p_N of period N , and define the rambling time for an initial point q as the integer $r_d(q)$ such that for all integers $i \geq r_d(q)$ and $k < r_d(q)$,

$$\begin{aligned} \max\{|T^i(q) - T^j(p_N)| \mid 0 \leq j < N\} &\leq d \\ \max\{|T^k(q) - T^j(p_N)| \mid 0 \leq j < N\} &> d. \end{aligned}$$

If the threshold value is too large, we may obtain a number of iterations that do not make orbits converge to periodic points. On the contrary, too small threshold value causes an overestimation of rambling time. When Lyapunov multiplier of the sink has an absolute value near one, in particular, at parameters near saddle-node bifurcation and period-doubling bifurcation, the rate of convergence of orbits is slow and therefore the overestimation of rambling time is large.

How to determine the appropriate threshold value is the following. Let α and β be eigenvalues of $DT^N(p_N)$ and let Lyapunov multiplier $|\Lambda|$ be $\max\{|\alpha|, |\beta|\}$, where $DT^N(p_N)$ is the Jacobian matrix of N th iteration of Hénon map T at the stable periodic point p_N . Obviously, $|\Lambda|$ is less than one because p_N is stable. For sufficient small threshold values d_0 and d_1 such that $d_1 < d_0$, we denote rambling times for some initial point q by r_0 and r_1 respectively. Then, because the distance from the orbit of the stable periodic point decreases approximately at the rate $|\Lambda|^{1/N}$ at every iteration in the neighborhood of the periodic point, we have

$$\frac{d_1}{d_0} \approx |\Lambda|^{(r_0 - r_1)/N}.$$

Therefore,

$$\frac{r_0 - r_1}{\log d_0 - \log d_1} \approx -\frac{N}{\log |\Lambda|}.$$

We take about 10000 uniformly distributed initial points in $[-1.5, 1.5] \times [-1.0, 1.0]$ and calculate averages of all values of rambling time. For various threshold values, we calculate values of average rambling time. The result shown as the graph in Fig. 13, which is the relation between logarithms of

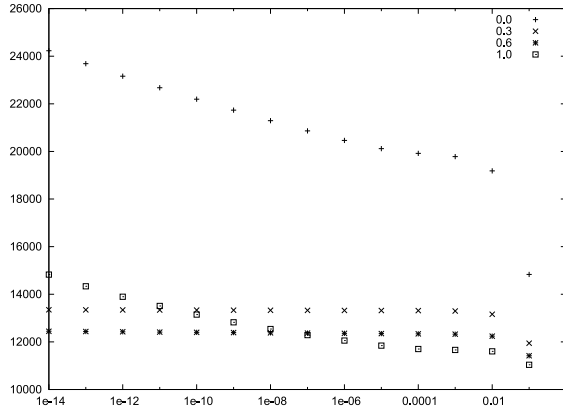


Figure 13. Relation of average rambling time and various threshold values for parameters where the sink of period 8 exists. The horizontal axis means threshold values with log scale and the vertical axis means average rambling time. The numbers 0.0, 0.3, 0.6, and 1.0 on the horizontal axis are fractions in the parameter interval. The number 0.0 means a parameter just after saddle-node bifurcation and the number 1.0 means a parameter just before period-doubling bifurcation.

threshold distance and average rambling time. As stated above, for sufficient small thresholds, the rate of contraction is constant and the graph has the constant slope whose absolute value is almost $N/\log |\Lambda|$. Therefore, the threshold value at the change of the slope is appropriate. From the graph we take 10^{-6} as the appropriate threshold value for the sink of period 8.

We calculated average rambling time for the sinks of period from 8 to 15. Each parameter is at the middle value of the parameter interval when each sink persists. We plot the sizes of parameter intervals of the periodic windows and the logarithms of values of average rambling time and obtain Fig. 14. From (16) we consider fitting

$$\log \tau = -\beta \log \Delta a + \gamma$$

for some constants β and γ with the graph in 14. Our obtained fitting parameter β is -0.902897 and this value agrees with the value for the case of large periodic window, that is, the case of sinks of lower period, investigated in [3]. As for average rambling time, the sinks that we obtained have the same scaling property as that of the sinks of lower period.

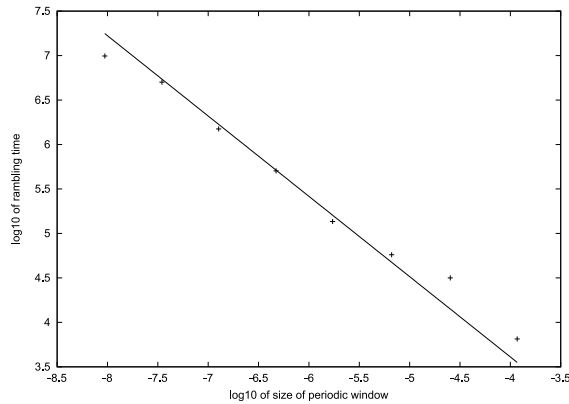


Figure 14. Logarithms to base 10 of average rambling time and size of periodic window. Average rambling time is calculated at a center of parameter interval from saddle-node bifurcation to period-doubling bifurcation. The points from left to right corresponds to sinks of periods 15, 14, 13, 12, 11, 10, 9, and 8. We can seem to fit the relation with linear mapping. The slope of the linear mapping is -0.902897 .

Acknowledgments The author would like to thank Professor Kenji Matsumoto for all of his guidance and advice.

Appendix A. Appendix

A.1. Algorithm: search for a sink near a homoclinic tangency

We show the algorithm to search for a sink near a parameter value that a homoclinic tangency occurs. Here, we search for a sink when two transversal homoclinic points exists after the homoclinic tangency. Let f be the diffeomorphism of surfaces that satisfies such a condition. Note that sinks may exist before the homoclinic tangency occurs, that is, at parameters such that there is no homoclinic point near the tangency. In that case, the same algorithm can find sinks by determining suitable search region at the opposite side.

In advance, we find the search region like the Fig. 15, in which the unstable manifold stick a little out of the stable manifold. We take a parallelogram so that its two vertexes are homoclinic points and it includes the curve of unstable manifold between the two homoclinic points. Here we fix the parameter value near the tangency and let this parallelogram be $ABCD$, where C and D are the homoclinic points. If we find a period m of periodic

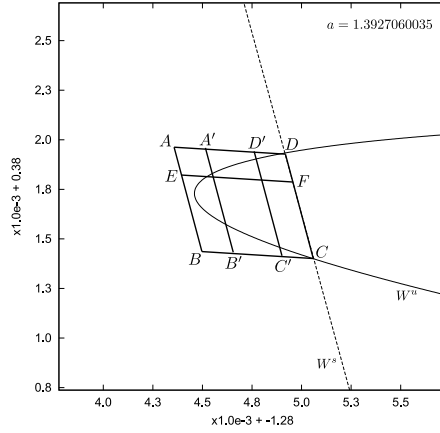


Figure 15. The parameters of map (1) are $a = 1.3927060035$ and $b = -0.3$. The points D and C are homoclinic points: the intersections of the stable and unstable manifolds for the saddle periodic point. The parallelogram $ABCD$ includes the segment of the unstable manifold from D to C . The lines AD , EF , and BE are parallel to each other. The lines AB , DC , $B'C'$, and $D'E'$ are parallel to each other. In $ABCD$ there is a periodic saddle point of period 13.

point and a parallelogram $A'B'C'D'$ satisfying the following conditions:

- (1) A' and D' are on AD and B' and C' are on BC ,
- (2) $A'B'$ is parallel to AB and $C'D'$ is parallel to CD ,
- (3) the intersection of the parallelogram $A'B'C'D'$ and the region $f^m(A'B'C'D')$ has two components; that is, there is a horseshoe,

we proceed to the next step, where we calculate approximate coordinates of two saddle periodic points of period m in the intersection of $A'B'C'D'$ and $f^m(A'B'C'D')$. If we can not obtain m and $A'B'C'D'$ satisfying the conditions, We repeat perturbing the parameter and trying to find them until they are found.

We want to obtain two periodic points of period m in $ABCD$. We fix the line segment EF parallel to AD and map the line m times. $f^m(EF)$ is alike the shape of the unstable manifold. Then we calculate the point of the intersection of EF and $f^m(EF)$ and let q be the intersection point. We determine whether $f^m(q)$ is on the AD side from EF or the BC side from EF . To change the position of line EF and repeat this procedure, we divide AB and CD with sufficiently small size and then obtain points E_1, \dots, E_k and F_1, \dots, F_k such that $E_i F_i$ is parallel to AD for all i . For

$E_i F_i$ we calculate the intersection q_i by the above procedure. Then we pick up a pair of points (q_-, q_+) from q_i so that q_- and q_+ are mapped to the different side from EF . We shorten the distance of two points q_- and q_+ by bisection method and obtain a sufficiently short line segment between q_- and q_+ . Then the midpoint of q_- and q_+ approximates point of periodic point. In the case that the condition (3) is satisfied, we obtain two saddle periodic points.

One of the two saddle periodic points becomes a sink when the intersection of a suitable parallelogram $A'B'C'D'$ and $f^m(A'B'C'D')$ consists of one component at a parameter nearer to the tangency. Although there is not necessarily a periodic point in such a case, if we find a pair of (q_-, q_+) then we obtain approximate coordinate of a periodic point. We repeat searching for periodic points until we take suitable parameter and the obtained periodic point is a sink.

A.2. Pseudo code of search for periodic points in a horseshoe

The algorithm in Appendix A.1 to search for periodic points in the search region $ABCD$ is expressed by the following pseudo code.

```
def q_and_direction(EF)
  q = (an intersection of EF and f^m(EF))
  tmp, distance_q = projection(DA, DC, q - D)
  tmp, distance_fq = projection(DA, DC, f^m(q) - D)
  return [q, distance_fq - distance_q]
end

def calc_periodic_point
  n = (sufficient large number of partition of AB and DC)
  error = (maximum distance of coordinates of periodic points)
  vector_step = (B - A) / n
  q_interval_data = []
  last = nil
  for i from 0 to n
    E = A + vector_step * i
    F = E + (D - A)
    q, direction = q_and_direction(EF)
    current = [E, q, direction]
    if last
```

```

E_last, q_last, direction_last = last
if direction > 0 && direction_last < 0
  q_interval_data.push [current, direction_last]
else if direction < 0 && direction_last > 0
  q_interval_data.push [direction_last, current]
end
end
last = current
end
if q_interval_data.empty?
  return nil
end
periodic_points = []
for data_plus, data_minus in q_interval_data
  E_plus, q_plus, direction_plus = data_plus
  E_minus, q_minus, direction_minus = data_minus
  while (q_plus - q_minus).abs > error
    E = (E_plus + E_minus) / 2
    F = E + (D - A)
    q, direction = q_and_direction(EF)
    if direction > 0
      E_plus, q_plus = E, q
    else
      E_minus, q_minus = E, q
    end
  end
  periodic_points.push ((q_plus + q_minus) / 2)
end
return periodic_points
end

```

A.3. Lists of coordinates and parameters of sinks

The coordinates, parameters, and eigenvalues of sinks that we found are listed in Table 2, Table 3, Table 4, Table 5, and Table 6. The parameter ranges where the sinks persist are listed in Table 7 and 8.

Table 2. The values of parameter a where the sink exists.

| period | a | period | a |
|--------|------------------------|--------|------------------------|
| | | 8 | 1.38664149787356250000 |
| 9 | 1.39682967781508590995 | 10 | 1.39044451080738447805 |
| 11 | 1.39348183318325079174 | 12 | 1.39187124135913547473 |
| 13 | 1.39270603514708815022 | 14 | 1.39227051835401997070 |
| 15 | 1.39249759396078376854 | 16 | 1.39237923569364948177 |
| 17 | 1.39244095493338897575 | 18 | 1.39240878086818029898 |
| 19 | 1.39242555647987797736 | 20 | 1.39241681068117711904 |
| 21 | 1.39242137052683480445 | 22 | 1.39241899322602361400 |
| 23 | 1.39242023267157798334 | 24 | 1.39241958647359244535 |
| 25 | 1.39241992337792816159 | 26 | 1.39241974772878703645 |
| 27 | 1.39241983930576794529 | 28 | 1.39241979156096093336 |
| 29 | 1.39241981645332931688 | 30 | 1.39241980347537751260 |
| 31 | 1.39241981024159838398 | 32 | 1.39241980671394307857 |
| 33 | 1.39241980855313113200 | 34 | 1.39241980759424702657 |
| 35 | 1.39241980809417346952 | 36 | 1.39241980783353045237 |
| 37 | 1.39241980796942000901 | 38 | 1.39241980789857225808 |
| 39 | 1.39241980793550963533 | 40 | 1.39241980791625186329 |
| 41 | 1.39241980792629214800 | 42 | 1.39241980792105751770 |
| 43 | 1.39241980792378665887 | 44 | 1.39241980792236378636 |
| 45 | 1.39241980792310561907 | 46 | 1.39241980792271885514 |
| 47 | 1.39241980792292049944 | 48 | 1.39241980792281536962 |
| 49 | 1.39241980792287018039 | 50 | 1.39241980792284160409 |
| 51 | 1.39241980792285650271 | 52 | 1.39241980792284873513 |
| 53 | 1.39241980792285278485 | 54 | 1.39241980792285067348 |
| 55 | 1.39241980792285177427 | 56 | 1.39241980792285120036 |
| 57 | 1.39241980792285149957 | 58 | 1.39241980792285134357 |
| 59 | 1.39241980792285142491 | 60 | 1.39241980792285138250 |

Table 3. The coordinates of sinks of odd period.

| period | x | y |
|--------|-------------------------|------------------------|
| 9 | -1.27976154338630332676 | 0.38150016090627654680 |
| 11 | -1.27648733082531270876 | 0.38168343400248646793 |
| 13 | -1.27553716276434521174 | 0.38171016190532197212 |
| 15 | -1.27527703273885344572 | 0.38171694500136863446 |
| 17 | -1.27520623128411636160 | 0.38171877870769113704 |
| 19 | -1.27518697955868689668 | 0.38171927701715012326 |
| 21 | -1.27518174604472220710 | 0.38171941247399922304 |
| 23 | -1.27518032343168631819 | 0.38171944929478208728 |
| 25 | -1.27517993673462261571 | 0.38171945930346351249 |
| 27 | -1.27517983162267160731 | 0.38171946202402293808 |
| 29 | -1.27517980305121079612 | 0.38171946276352383767 |
| 31 | -1.27517979528493993763 | 0.38171946296453424263 |
| 33 | -1.27517979317391901322 | 0.38171946301917274315 |
| 35 | -1.27517979260010318583 | 0.38171946303402452279 |
| 37 | -1.27517979244412908254 | 0.38171946303806152270 |
| 39 | -1.27517979240173234159 | 0.38171946303915885577 |
| 41 | -1.27517979239020809754 | 0.38171946303945713191 |
| 43 | -1.27517979238707558788 | 0.38171946303953820909 |
| 45 | -1.27517979238622411191 | 0.38171946303956024741 |
| 47 | -1.27517979238599266448 | 0.38171946303956623785 |
| 49 | -1.27517979238592975265 | 0.38171946303956786617 |
| 51 | -1.27517979238591265201 | 0.38171946303956830877 |
| 53 | -1.27517979238590800373 | 0.38171946303956842908 |
| 55 | -1.27517979238590674024 | 0.38171946303956846178 |
| 57 | -1.27517979238590639680 | 0.38171946303956847067 |
| 59 | -1.27517979238590630344 | 0.38171946303956847309 |

Table 4. The coordinates of sinks of even period.

| period | x | y |
|--------|-------------------------|------------------------|
| 8 | -1.26414803155990566355 | 0.38158830955359902274 |
| 10 | -1.27259518279931735196 | 0.38177393058021936800 |
| 12 | -1.27449094519060074464 | 0.38173697294814371573 |
| 14 | -1.27499306560590518015 | 0.38172428819387392387 |
| 16 | -1.27512906462917220609 | 0.38172077592692207224 |
| 18 | -1.27516600565582752278 | 0.38171981987086304374 |
| 20 | -1.27517604505617454618 | 0.38171956002976662202 |
| 22 | -1.27517877380397668935 | 0.38171948940301306126 |
| 24 | -1.27517951551703021723 | 0.38171947020562793720 |
| 26 | -1.27517971712775127688 | 0.38171946498743782459 |
| 28 | -1.27517977192930977783 | 0.38171946356903620597 |
| 30 | -1.27517978682541319353 | 0.38171946318348788627 |
| 32 | -1.27517979087445722178 | 0.38171946307868536363 |
| 34 | -1.27517979197506578554 | 0.38171946305020205462 |
| 36 | -1.27517979227423197757 | 0.38171946304245888379 |
| 38 | -1.27517979235555106303 | 0.38171946304035414230 |
| 40 | -1.27517979237765514390 | 0.38171946303978203373 |
| 42 | -1.27517979238366345528 | 0.38171946303962652358 |
| 44 | -1.27517979238529662910 | 0.38171946303958425299 |
| 46 | -1.27517979238574055693 | 0.38171946303957276302 |
| 48 | -1.27517979238586122500 | 0.38171946303956963983 |
| 50 | -1.27517979238589402489 | 0.38171946303956879089 |
| 52 | -1.27517979238590294052 | 0.38171946303956856013 |
| 54 | -1.27517979238590536396 | 0.38171946303956849741 |
| 56 | -1.27517979238590602270 | 0.38171946303956848036 |
| 58 | -1.27517979238590620176 | 0.38171946303956847572 |
| 60 | -1.27517979238590625043 | 0.38171946303956847446 |

Table 5. The eigenvalues of Jacobian matrix at sinks of odd period.

| period | two eigenvalues | |
|--------|----------------------------|-----------------------------|
| 9 | 3.93390430424863572693e-05 | -5.00342623452793819690e-01 |
| 11 | 3.54263945135985294617e-06 | -5.00042418745157891713e-01 |
| 13 | 3.18857384659543061078e-07 | -5.00011314369376520844e-01 |
| 15 | 2.86978455992962120235e-08 | -4.99999449448285191163e-01 |
| 17 | 2.58280782017907830145e-09 | -4.99999117205112460657e-01 |
| 19 | 2.32453372758525399328e-10 | -4.99997678333266171675e-01 |
| 21 | 2.09207534187041027181e-11 | -4.99998876409870098498e-01 |
| 23 | 1.88287341702849328254e-12 | -4.99997386842789247998e-01 |
| 25 | 1.69458272154285856180e-13 | -4.99998376397685221343e-01 |
| 27 | 1.52512261305216089434e-14 | -4.99998978424838033738e-01 |
| 29 | 1.37261512953728858791e-15 | -4.99997238031453454875e-01 |
| 31 | 1.23535011654083814097e-16 | -4.99998654643368048328e-01 |
| 33 | 1.11181883091214677720e-17 | -4.99996979003748000016e-01 |
| 35 | 1.00063350481841684327e-18 | -4.99998699404722023775e-01 |
| 37 | 9.00573388519507224953e-20 | -4.99996903785086484289e-01 |
| 39 | 8.10514641651424309589e-21 | -4.99997772373598520888e-01 |
| 41 | 7.29461280737077233910e-22 | -4.99999072470535969690e-01 |
| 43 | 6.56516993188628512944e-23 | -4.99997670738468243304e-01 |
| 45 | 5.90862837774424798774e-24 | -4.99999749125990749627e-01 |
| 47 | 5.31778336629985726135e-25 | -4.99998073021506810272e-01 |
| 49 | 4.78601644841757988752e-26 | -4.99996880097932052687e-01 |
| 51 | 4.30739540375381064480e-27 | -4.99999132004147030989e-01 |
| 53 | 3.87667156874804492837e-28 | -4.99997106382157594747e-01 |
| 55 | 3.48898847864605526430e-29 | -4.99999389728043278690e-01 |
| 57 | 3.14009843056555073580e-30 | -4.99997988534170688869e-01 |
| 59 | 2.82608159221948370039e-31 | -4.99999226159685406967e-01 |

Table 6. The eigenvalues of Jacobian matrix at sinks of even period.

| period | two eigenvalues | |
|--------|-----------------------------|-----------------------------|
| 8 | -1.31756529641247091095e-04 | -4.97963935287655270780e-01 |
| 10 | -1.18133309069991084047e-05 | -4.99850554131307012274e-01 |
| 12 | -1.06293833396807615975e-06 | -4.99973500829598525112e-01 |
| 14 | -9.56602744063121882799e-08 | -4.99995325090181168966e-01 |
| 16 | -8.60239206305607819397e-09 | -5.00404081614332513694e-01 |
| 18 | -7.74841687665481002823e-10 | -4.99999542057756894204e-01 |
| 20 | -6.97359635462816038970e-11 | -4.99998024503659284505e-01 |
| 22 | -6.27623420560484567082e-12 | -4.99998224747187910007e-01 |
| 24 | -5.64859702331267123535e-13 | -4.99999442897710240236e-01 |
| 26 | -5.08373713413655108715e-14 | -4.99999461274412252093e-01 |
| 28 | -4.57537721971967473237e-15 | -4.99997953313292507077e-01 |
| 30 | -4.11784366413982750698e-16 | -4.99997447420475116763e-01 |
| 32 | -3.70901172093154857698e-17 | -4.99599442728760061741e-01 |
| 34 | -3.33543642932484048777e-18 | -4.99999986599725615837e-01 |
| 36 | -3.00189822904642170476e-19 | -4.99999080064342980871e-01 |
| 38 | -2.70171822400185678205e-20 | -4.99997263101728888163e-01 |
| 40 | -2.43153696864478972700e-21 | -4.99999202801879231238e-01 |
| 42 | -2.18839219844543512559e-22 | -4.99997163256385952844e-01 |
| 44 | -1.96954266299893654582e-23 | -4.99999782022565387678e-01 |
| 46 | -1.77259597084709034774e-24 | -4.99997645567087084226e-01 |
| 48 | -1.59533016931113382843e-25 | -4.99999590124442955948e-01 |
| 50 | -1.43580256269141808060e-26 | -4.99997706053783413257e-01 |
| 52 | -1.29222256964477301264e-27 | -4.99997604205504607867e-01 |
| 54 | -1.16299516649381451037e-28 | -4.99999816666042300859e-01 |
| 56 | -1.04669993898611976437e-29 | -4.9999776778890282377e-01 |
| 58 | -9.42030605056904756496e-31 | -4.99997417489607197743e-01 |
| 60 | -8.47823597101255199667e-32 | -4.99999745467728878269e-01 |

Table 7. The ranges of parameter a where the sinks of odd period persist.

| period | parameters at saddle-node and period-doubling bifurcations |
|--------|--|
| 9 | 1.39682334899770309745000000000000000000 1.39683459875008590995000000000000000000 |
| 11 | 1.3934814033585920161703076171875000000000 1.3934821674769293329915966796875000000000 |
| 13 | 1.3927060033907990877176504658789062500000 1.3927060598461127595926504658789062500000 |
| 15 | 1.3924975916102853082129492045595297082118 1.3924975957889620773495764018251547082118 |
| 17 | 1.3924409547595970907162926627654496057239 1.3924409550685610077582598531140747888294 |
| 19 | 1.3924255564670342362919272183792474599801 1.3924255564898676304460081461127433512680 |
| 21 | 1.3924213705258857640361478743510716334863 1.3924213705275729495745331210998578409123 |
| 23 | 1.3924202326715078614033818373402620991773 1.3924202326716325230348642628494487551308 |
| 25 | 1.3924199233779229805475791529833319211205 1.3924199233779321913146081892009110634698 |
| 27 | 1.3924198393057675624874615984039427609140 1.3924198393057682430321434709276059681053 |
| 29 | 1.3924198164533292885924061461208154283204 1.3924198164533293388749066755548266733108 |
| 31 | 1.3924198102415983818904458058059739853184 1.3924198102415983856056005794709084594730 |
| 33 | 1.3924198085531311318467143293844744895717 1.3924198085531311321212108966380177168874 |
| 35 | 1.3924198080941734695060031588558768691861 1.3924198080941734695262845103777038213962 |
| 37 | 1.3924198079694200090076905741665406453504 1.3924198079694200090091890743252826662156 |
| 39 | 1.3924198079355096353303997704166508400297 1.3924198079355096353305104880280764674629 |
| 41 | 1.3924198079262921480018356108329882157974 1.3924198079262921480018437912731663998231 |
| 43 | 1.3924198079237866588725607040184013057408 1.3924198079237866588725613084353430369478 |
| 45 | 1.3924198079231056190671970667612411855520 1.3924198079231056190671971114189552419361 |
| 47 | 1.3924198079229204994388359115639426542337 1.3924198079229204994388359148635064731155 |
| 49 | 1.3924198079228701803876815565029861453483 1.3924198079228701803876815567467764674448 |
| 51 | 1.3924198079228565027083804295458118884747 1.3924198079228565027083804295638244883347 |
| 53 | 1.3924198079228527848538745792375525219619 1.3924198079228527848538745792388833941745 |
| 55 | 1.3924198079228517742700012221913783310748 1.3924198079228517742700012221914766633938 |
| 57 | 1.3924198079228514995740002134887019719025 1.3924198079228514995740002134887092372474 |
| 59 | 1.3924198079228514249063798807901536743561 1.3924198079228514249063798807901542111607 |

References

- [1] Arai Z. and Mischaikow K., *Rigorous computations of homoclinic tangencies*. SIAM J. Appl. Dyn. Syst. **5** (2006), 280–292.
- [2] Buszko K. and Stefański K., *Transient dynamics inside periodic windows and in their vicinity i. logistic maps*. Open Syst. Inf. Dyn. **10** (2003), 183–203, 10.1023/A:1024614307468.
- [3] Buszko K. and Stefański K., *Measuring transient chaos in nonlinear one- and two-dimensional maps*. Chaos, Solitons & Fractals **27**(3) (2006), 630–646.
- [4] Curry J. H. and Johnson J. R., *On the rate of approach to homoclinic tangency*. Physical letters **92**(5) (1982), 217–220.
- [5] Fornæss J. E. and Gavosto E. A., *Existence of generic homoclinic tangencies for Hénon mappings*. J. Geom. Anal. **2**(5) (1992), 429–444.
- [6] Gavrilov N. K. and Silnikov L. P., *On three-dimensional dynamical systems close to systems with a structurally unstable homoclinic curve. i*. Mathematics of the USSR - Sbornik **17** (1972), 467–485.
- [7] Grebogi C., Ott E. and Yorke J. A., *Basin boundary metamorphoses: changes in accessible boundary orbits*. Physica D **24** (1987), 243–262.
- [8] Hénon M., *A two-dimensional mapping with a strange attractor*. Comm. Math. Phys. **50**(1) (1976), 69–77.
- [9] Jacobs J., Ott E. and Hunt B. R., *Scaling of the durations of chaotic transients in windows of attracting periodicity*. Phys. Rev. E **56**(6) (1997), 6508–6515.
- [10] Moore R. E., *Methods and Applications of Interval Analysis*. SIAM Studies in Applied Mathematics, 1979.
- [11] Newhouse S. E., *Diffeomorphisms with infinitely many sinks*. Topology **13** (1974), 9–18.
- [12] Newhouse S. E., *The abundance of wild hyperbolic sets and non-smooth stable sets for diffeomorphisms*. Publications mathématiques de l’I.H.É.S. **50** (1979), 101–151.
- [13] Robinson C., *Bifurcation to infinitely many sinks*. Comm. Math. Phys. **90**(3) (1983), 433–459.
- [14] Tatjer J. C. and Simó C., *Basins of attraction near homoclinic tangencies*. Ergodic Theory Dynam. Systems **14**(2) (1994), 351–390.
- [15] Tedeschini-Lalli L. and Yorke J. A., *How often do simple dynamical processes have infinitely many coexisting sinks?* Comm. Math. Phys. **106**(4) (1986), 635–657.
- [16] Yorke J. A. and Alligood K. T., *Period doubling cascades of attractors: a prerequisite for horseshoes*. Comm. Math. Phys. **101**(3) (1985), 305–321.

Department of Mathematics
Hokkaido University
Sapporo 060-0810, Japan
E-mail: yt@math.sci.hokudai.ac.jp